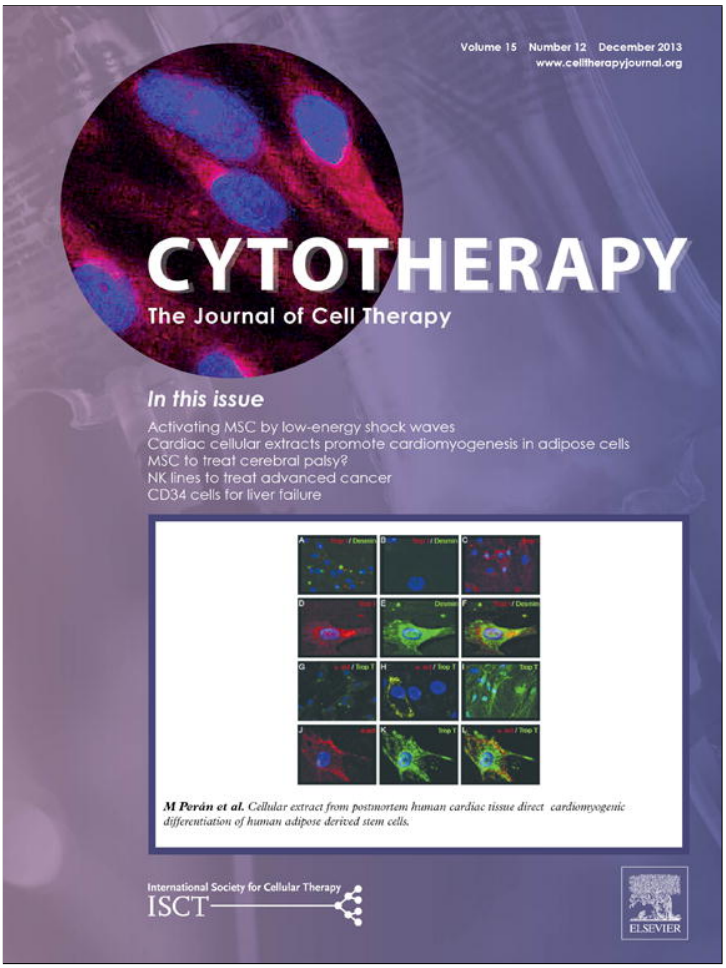

Cytotherapy, 2013; 15: 1484–1497

International Society for Cellular Therapy ISCT®

Immortalized human fetal bone marrow-derived mesenchymal stromal cell expressing suicide gene for anti-tumor therapy *in vitro* and *in vivo*

WAYNE Y. W. LEE[1], TING ZHANG[1], CAROL P. Y. LAU[1], C. C. WANG[2], KAI-MING CHAN[1] & GANG LI[1,3,4]

[1]*Departments of Orthopaedics and Traumatology and* [2]*Obstetrics and Gynaecology and* [3]*Stem Cells and Regeneration Program, School of Biomedical Sciences, Li Ka Shing Institute of Health Sciences, and* [4]*MOE Key Laboratory of Regenerative Medicine, School of Biomedical Sciences, The Chinese University of Hong Kong, Shatin, Hong Kong SAR, China*

Abstract

Background aims. Cancer is one of the greatest health challenges facing the world today with >10 million new cases of cancer every year. The self-renewal, tumor-homing ability and low immunogenicity of mesenchymal stromal cells (MSCs) make them potential delivery candidates for suicide genes for anti-tumor therapy. However, unstable supply and short life span of adult MSCs *in vitro* have limited this therapeutic potential. In this study, we aimed to evaluate if immortalization of human fetal bone marrow-derived mesenchymal stromal cells by simian virus 40 (SV40-hfBMSCs) could be a stable source of MSCs for clinical application of suicide gene therapy. *Methods and Results.* Transduction of SV40 and herpes simplex virus thymidine kinase-IRES-green fluorescent protein (TK-GFP) did not cause significant change in the stem cell properties of hfBMSCs. The anti-tumor effect of SV40-TK-hfBMSCs in the presence of the prodrug ganciclovir was demonstrated *in vitro* and in nude mice bearing human prostate cancer cells, DU145 and PC3, which had been transduced with luciferase and GFP for imaging evaluation by an *in vivo* live imaging system (IVIS 200 imaging system; Caliper Life Sciences). Repeated injection of low doses (1×10^6 cells/kg) of SV40-TK-hfBMSCs was as effective as previously reported and did not cause observable harmful side effects in multiple organs. Mixed lymphocyte reaction showed that SV40-TK-hfBMSCs did not induce significant proliferation of lymphocytes isolated from healthy adults. *Conclusions.* Taken together, immortalized hfBMSCs represent a reliable and safe source of MSCs for further clinical translational study.

Key Words: *fetal mesenchymal stromal cells, ganciclovir, prostate cancer, simian virus 40, thymidine kinase*

Introduction

Mesenchymal stromal cells (MSCs) are characterized on the basis of colony-forming ability, multilineage differentiation potency and expression of particular surface phenotypes (1). MSCs secrete diverse immunomodulatory and trophic bioactive factors at sites of injury (2), which contribute to their therapeutic potential in various conditions such as myocardial infarction and cartilage damage (3). Cumulative evidence revealed the immuno-privilege and immunomodulatory properties of MSCs (4–6), which support the therapeutic use of allogeneic MSCs in immune-associated disorders. Data from clinical studies using MSCs for the treatment and prevention of graft-versus-host disease revealed its safety regardless of the variation of human leukocyte antigen (7). These findings point to a strategic use of pre-manufactured MSCs with quality and sterility assurance to reduce time constraints and increase the accessibility of MSCs when allogeneic MSCs are not applicable because of emergency or inherited genetic disorders.

Tumor sites are regarded as a microenvironment with hypoxia and inflammation with the release of many cytokines that attract MSCs. This tumor-tropic homing capability and inhibitory effect on tumorigenesis provide a strong rationale for the use of systemic injected MSCs for the treatment of tumors that are not easily accessible (8,9) and for engineering MSCs into vehicles of anti-tumor agents. Enzyme-activated prodrug therapy is one transgene strategy (10). It was primarily used in virus-mediated

Correspondence: Prof **Gang Li**, Room 904, Li Ka Shing Institute of Health Sciences, The Chinese University of Hong Kong, Prince of Wales Hospital, Shatin, Hong Kong SAR. E-mail: gangli@cuhk.edu.hk

(Received 5 February 2013; accepted 19 June 2013)

ISSN 1465-3249
http://dx.doi.org/10.1016/j.jcyt.2013.06.010

gene therapy (11) and later adopted using MSCs as the vector (12). Thereafter, we and other groups reported and consolidated the anti-tumor effect of this therapeutic approach via other suicide genes, such as herpes simplex virus thymidine kinase (TK) and caspase 9 (13,14). Suicide genes are of particular interest because they facilitate the development of MSCs in anti-tumor therapy as MSCs are also reported to play dual roles in tumorigenesis through potentiating tumor growth, enhancement of neovascularization or differentiating into tumor stromal fibroblasts (15–17). This therapy reduces the risk of MSC-promoted tumorigenesis. MSC expressing TK (MSC-TK) with its prodrug ganciclovir (GCV) (MSC-TK-GCV) has been used in attempts to treat pancreatic tumor, hepatocellular carcinoma, glioblastoma, prostate tumor and metastatic lung tumor in animal models (14,18–21). In these studies, the effective dosage of MSC-TK ranged from 0.5×10^6 to 1×10^6 per mice. Without consideration of interspecies differences, the dosage to be used in human patients would be estimated to be 2×10^7 to 4×10^7 per kg. Despite the promising outcome, the clinical application of the MSC-TK-GCV system is restricted by limited passaging capacity of MSCs and insufficient number of cells available for transfusion. A previous study demonstrated that proliferation of human adult bone marrow-derived mesenchymal stromal cells (BMSCs) stopped at 40 days after isolation (22). Also, the current protocol requires in-house transgene introduction, which may not be feasible in all medical centers. Previous studies demonstrated efficient expansion of MSCs without compromise in plasticity after introduction of a growth-promoting gene, such as human telomerase reverse transcriptase gene (23) or the embryonic fibroblasts modified by simian virus 40 large T antigen (SV40) (24). In this study, given that BMSCs isolated from human first-trimester bone marrow were comparatively more expandable than their adult counterparts owing to longer telomere length and greater telomerase and telomerase reverse transcriptase activities (25), we proposed a novel cellular system in which SV40 and TK were transduced into human fetal BMSCs (hfBMSCs), which has the potential to be a therapeutic agent in an off-the-shelf manner.

Methods

Cell culture

Human prostate cancer cell lines, DU145 and PC3, were obtained from the American Type Culture Collection (Manassas, VA, USA). Human embryonic kidney cell line, 293FT, was obtained from Life Technologies (Carlsbad, CA, USA). DU145 and PC3 were cultured in RPMI-1640 medium supplemented with 10% fetal bovine serum (FBS) and 1% penicillin and streptomycin (P/S). 293FT was cultured in high-glucose Dulbecco's modified Eagle's medium (DMEM) supplemented with 10% FBS and 1% P/S. Two sources of human tissues, human fetal bone tissues and human adult bone marrow aspirate, were used for the isolation of BMSCs. The use of human fetal tissues and human adult tissues was approved by Joint CUHK-NTEC Clinical Research Ethics Committee (ethical approval code CRE-2011.383 and CRE-2010.248, respectively). Fetal limbs, clinical specimens of surgical termination of pregnancy, were collected in the operating room, transported to clean room (International Organization for Standardization class 7; certified by National Environmental Balancing Bureau) and immersed in Dulbecco's phosphate-buffered saline (DPBS) containing 10% P/S during removal of surrounding tissues, muscles and vessels under a dissecting microscope (Nikon, Tokyo, Japan). The tissues were washed thoroughly with DPBS twice and cut into small pieces and cultured in Knockout DMEM (Life Technologies, Cell Treatment Therapy grade; CTS) supplemented with 10% FBS, 1% P/S (CTS) and 1% glutamax (CTS). For the adult bone marrow aspirate, MSCs were isolated by gradient centrifugation in LymphoPrep (Axis-Shield PoC AS, Oslo, Norway) as previously reported (14). The mononuclear cells were cultured in α-MEM supplemented with 10% FBS and 1% P/S. At confluence, the cells were trypsinized by TrypLE (CTS), and subjected to either passaging or cryopreserved in low dimethyl sulfoxide (DMSO, cell culture grade; Sigma-Aldrich, St. Louis, MO, USA) freezing medium (30% FBS, 5% DMSO and 1% glutamax) adopted from Texas A&M Institute for Regenerative Medicine. These two cells were subjected to MSC characterization and named human fetal BMSC (hfBMSC) and human adult BMSC (haBMSC), respectively. Reagents for cell culture were purchased from Life Technologies. Unless otherwise specified, all chemicals were purchased from Sigma-Aldrich.

Lentiviral transduction and MSC characterization

DU145 and PC3 expressing luciferase and GFP (i.e., Luc-GFP-DU145 and Luc-GFP-PC3) were developed in our previous study (14). For gene transduction in hfBMSCs, lentiviral particles were generated in 293FT cells using transient co-transfection of a four-plasmid lentiviral system. At 60% confluence, calcium phosphate transfection of transfer vector plasmid (either pLenti CMV/TO SV40 small + Large T or pLOX-GFP-IRES-TK) DNA (8 μg) (Addgene), helper plasmid plp-1 DNA (5.28 μg), plp-2 DNA

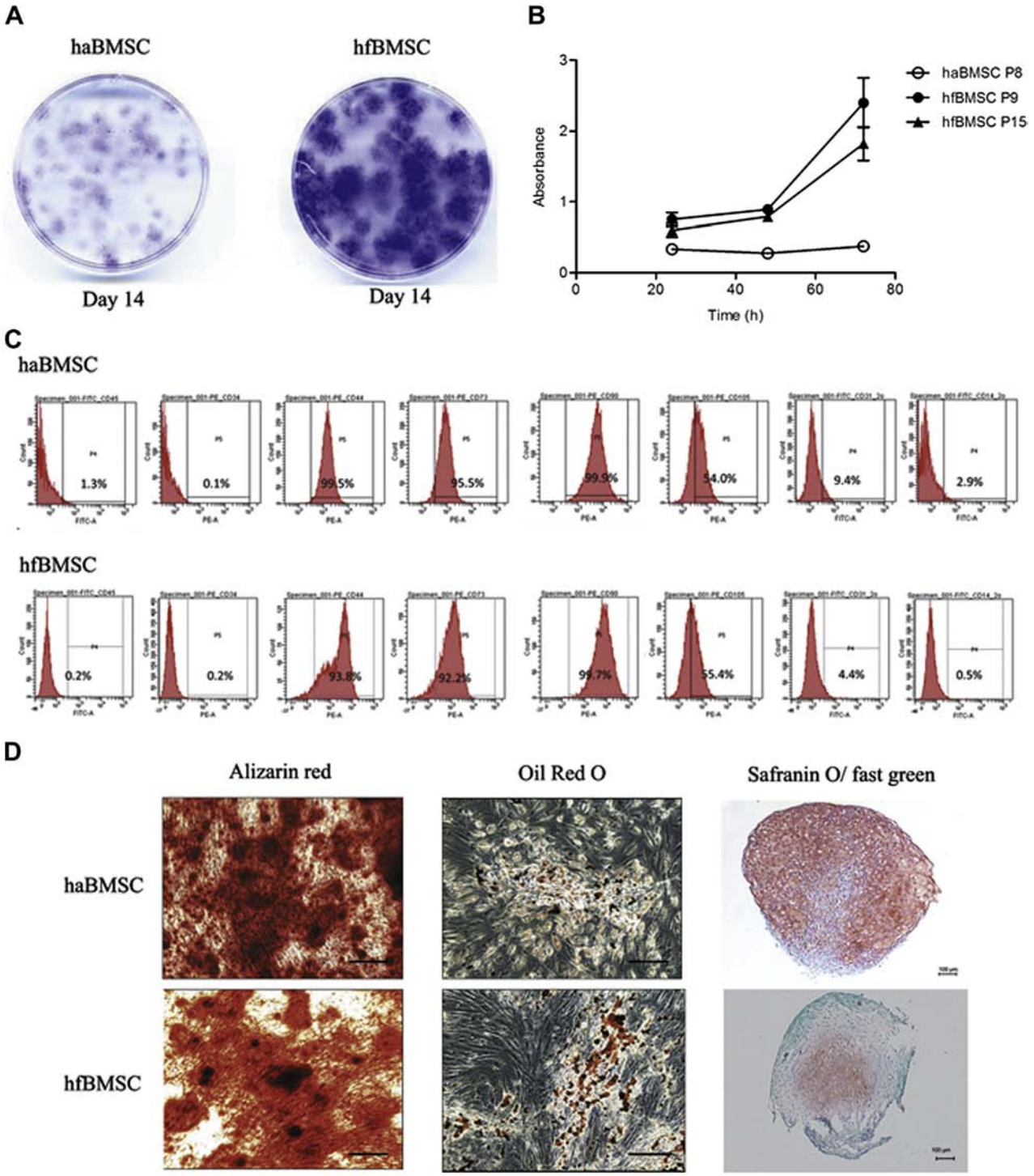

Figure 1. Stem cell properties of hfBMSCs. (A) Crystal violet staining of colony-forming assay of haBMSCs and hfBMSCs after 14 days of incubation at low-density plating. (B) BrdU assay showing slower proliferation of haBMSCs compared with hfBMSCs. The proliferation rate of hfBMSCs was similar at passage 9 and passage 15. (C) Flow cytometry data showing the expression of CD45, CD34, CD44, CD73, CD90, CD105, CD31 and CD14 on haBMSCs and hfBMSCs early at passage 2. The expression profiles were similar between the two MSCs, which were positive for CD44, CD73, CD90 and CD105 and negative for CD14, CD31, CD34 and CD45. (D) Staining of osteogenic differentiation by alizarin red, adipogenic differentiation by oil red O, and chondrogenic differentiation by safranin O and fast green. haBMSCs and hfBMSCs exhibited similar osteogenic and adipogenic differentiation potential, but hfBMSCs were more capable of undergoing chondrogenic differentiation as indicated by the expression level of proteoglycan in red.

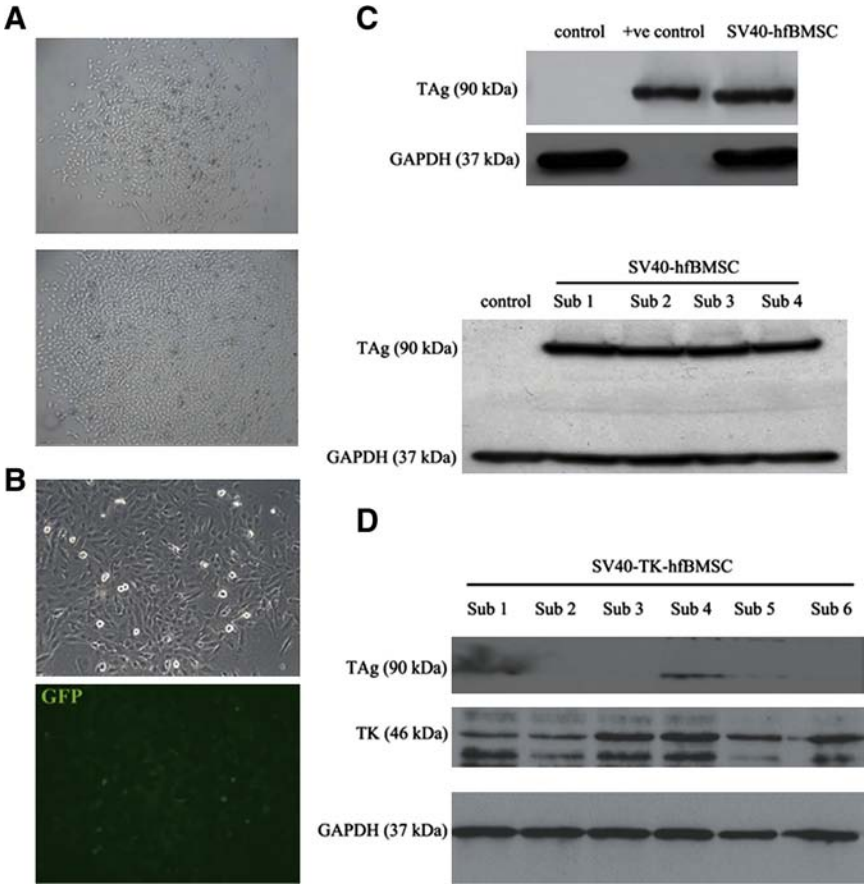

Figure 2. Transduction of hfBMSCs and evaluation of the expression of transgenes. (A) Single colony formed from SV40 transduced hfBMSCs in bright field. (B) Single colony formed from TK-GFP transduced SV40-hfBMSCs in bright field (upper panel) and fluorescent light (lower panel). (C) Single colonies of SV40-hfBMSCs were selected with the help of cloning ring, then subjected to Western blot for the determination of the expression of SV40. A SV40-expressing rat BMSC cell line was used as positive control. Four subclones of SV40-hfBMSCs were identified, and one of them was randomly selected for subsequent TK-GFP transduction. (D) The subclones of SV40-hfBMSCs were transduced further with TK-GFP. Subclones 1 and 4 were found to have expression of both SV40 and TK, whereas the expression of SV40 in subclones 2, 3, 5 and 6 were lost for unknown reasons. Subclone 4 with the highest expression level of SV40 and TK was selected for subsequent characterization and functional studies. Glyceraldehyde-3-phosphate dehydrogenase was used as loading reference in Western blot.

(4 μg) and envelop plasmid plp-VSV DNA (2.8 μg) (Life Technologies) was carried out; medium was changed after 12 h. Media containing viral particles were collected every 24 h in the following 3 days and concentrated using polyethylene glycol 6000 as previously described (26). To determine the lentiviral titer, p24 enzyme-linked immunosorbent assay was carried out according to the manufacturer's instruction (Cell Biolabs, Inc). Gene transduction was performed at 50 multiplicities of infection in the presence of 8 μg/mL hexadimethrine bromide (Polybrene, Sigma-Aldrich). Transduction was confirmed by Western blot using anti-TK (Santa Cruz Biotechnology) and anti-SV40 (BD Biosciences) antibodies. The stem cell properties of hfBMSCs with or without transduction were determined by colony-forming ability test, flow cytometry for surface phenotypes and multi-lineage differentiation potential as previously described (27) except that all antibodies used for flow cytometry were purchased from BD Biosciences.

Hydroxyapatite-tricalcium phosphate (HA-TCP) cell implantation in vivo

To allow cell attachment, 1×10^6 hfBMSCs were mixed with 40 mg of HA/TCP scaffold (Bicomposites) for 2 h. The cell scaffolds were then implanted subcutaneously in the dorsal sides of 12-week-old male nude mice (four scaffolds per mice). At 8 weeks after implantation, the implants were harvested, fixed with 10% neutral buffered formalin, decalcified with 9% formic acid for 3 weeks and embedded in paraffin for histologic examination.

Cell proliferation assay

For cell proliferation assay, 2×10^3 cells were plated in 96-well plates and cultured for 24, 48 and 72 h. Bromodeoxyuridine (BrdU) incorporation assay was carried out according to the manufacturer's manual (Roche Diagnostics). Optical density was

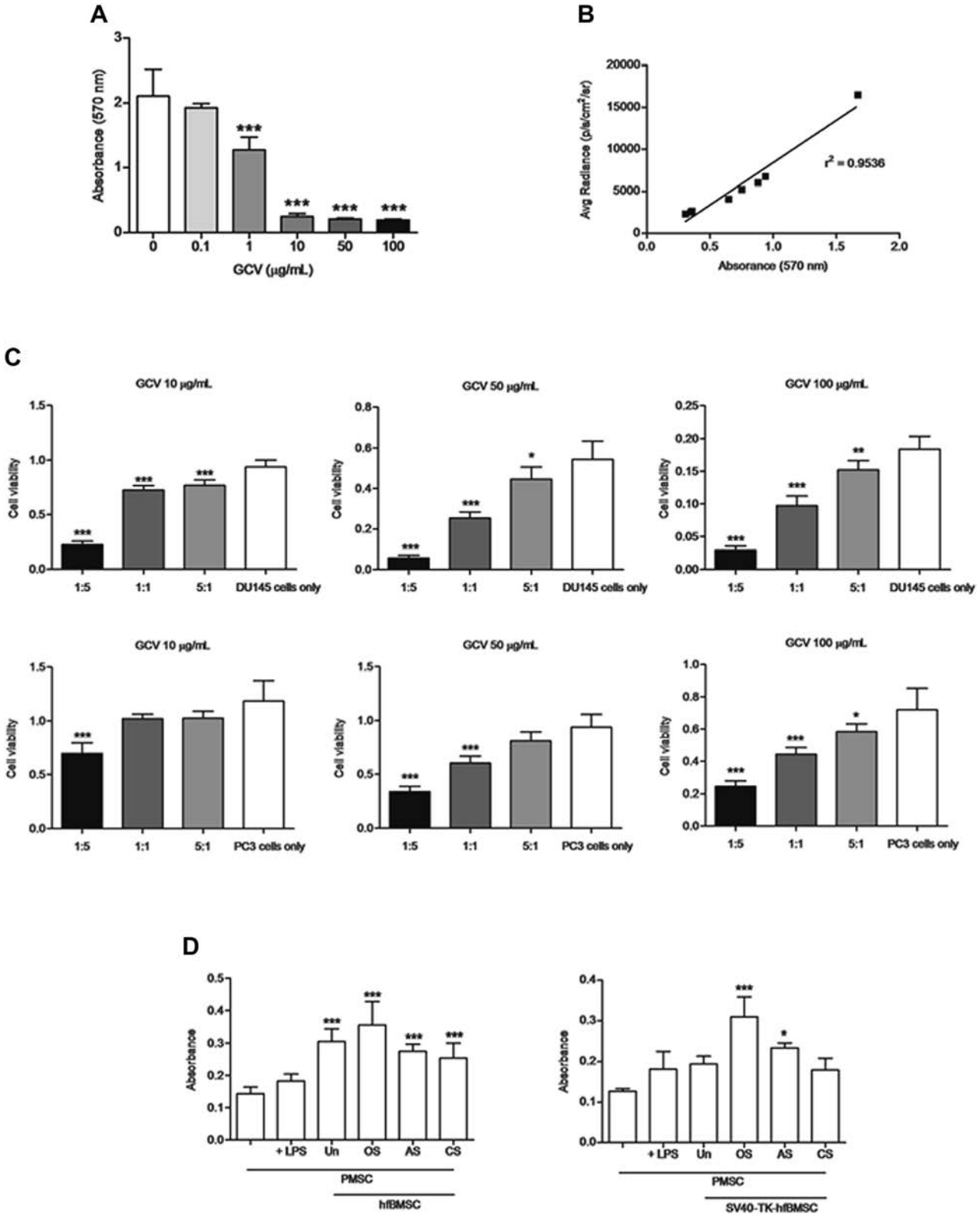

Figure 3. Functional assessment of the transduced TK transgene and immunogenicity study. (A) Functional expression of the transduced TK transgene was evaluated by the treatment of GCV at various concentrations for 6 days by MTT assay. Significant concentration-dependent reduction in absorbance was shown at $\geq$1 μg/mL. (B) In subsequent co-culture cytotoxicity experiments, the cytotoxic effects of TK/GCV on luciferase-expressing cancer cells were evaluated by bioluminescent signal acquired by IVIS 200. The quantitative signal intensity in the region of interest with fixed dimension along was expressed as photons per second per centimeter squared per steradian (a steradian is a unit of solid angle). A strong correlation was found between MTT assay and bioluminescent imaging, indicating that the results obtained from both were comparable. (C) Cytotoxic effect of TK/GCV treatment on Luc-GFP-DU145 or Luc-GFP-PC3 was shown

measured at 450 nm with reference wavelength at 690 nm.

Cell migration assay

For cell migration assay, 2×10^5 Luc-GFP-DU145 or Luc-GFP-PC3 cells were plated on bottom chambers of 24-well plates containing 600 μL completed RPMI-1640; 24 h later, 5×10^4 hfBMSCs were plated on transwell inserts with 600 μL completed Knockout DMEM and cultured for 1 h. Medium in bottom chambers was changed to completed Knockout DMEM, and transwell inserts with cells only were placed on corresponding bottom chambers and cultured for another 16 h. Remaining cells on the upper surface of the transwell inserts were removed with cotton swabs, and cells that migrated to the lower surface were fixed with 4% formaldehyde and then stained with 0.5% crystal violet solution. Air-dried inserts were cut and mounted on glass slides, and five random fields were taken for semi-quantitative analysis.

Mixed human peripheral blood lymphocyte reaction

For mixed human peripheral blood lymphocyte reaction, 5, 10 or 20×10^3 hfBMSCs were plated on 96-well plates. After 24 h, osteogenic, adipogenic or chondrogenic induction medium was added with normal completed medium as control for another 7 days. During the induction period, 2.5 μg/mL mitomycin C was added. The cells were then washed twice with DPBS, and 1×10^5 human peripheral blood lymphocytes (hPBLs, responders) isolated from healthy donors were added into each well. hfBMSC culture without hPBLs served as negative control, hPBLs alone served as baseline control, and hPBLs treated with 100 ng/mL lipopolysaccharide for 18 h served as positive control. After an additional 5 days of culture, the proliferation of hPBLs was determined by BrdU assay as previously described.

GCV-induced cytotoxicity in vitro

Cytotoxicity was determined by both MTT assay and bioluminescent imaging of luciferase activity (Sigma-Aldrich). In brief, cells at desired number were plated on 96-well plates and cultured overnight. GCV was added into the cells for desired incubation time. At the end of incubation, the GCV-containing medium was replaced by completed Knockout DMEM with 150 μg/mL D-Luciferin (Biosynth AG). The cell viability represented by luciferase activity was measured 10 min after incubation at 37°C and quantified by the IVIS 200 imaging system (Caliper Life Sciences). The cells were then subjected to MTT assay if needed according to experimental design. In the MTT assay, the culture medium was replaced by completed Knockout DMEM with 0.5 mg/mL MTT. The medium was removed 3 h after incubation at 37°C, and formazan precipitate was dissolved by addition of 100 μL DMSO. Optical density was measured by a microplate reader at 570 nm.

Tumor xenograft experiments

Subcutaneous injection of 5×10^6 cells of Luc-GGFP-DU145 or Luc-GFP-PC3 was performed at the dorsal site of nude mice (20–25 g). The viability of the injected cells was determined by IVIS 200 after intraperitoneal injection of D-Luciferin (30 mg/mL; 5 μL/g). The mice were subjected to MSC-GCV treatment 10 days after injection of cancer cells. A 3-day recovery window was given before and after each MSC injection (1×10^6/kg, intravenously). For every round of treatment, 30 mg/kg GCV was given intraperitoneally for 5 consecutive days. The change in tumor size along the treatment was measured by caliper and calculated as length $\times$ width^2/2, and assessed *in vivo* by live imaging with IVIS-200.

Immunohistochemistry and immunofluorescent staining

Tissues were embedded in either paraffin or ornithine carbamoyltransferase compound (Tissue-Tek, Sakura) for either paraffin or frozen sectioning. Both tissues were cut in 5-μm sections. For paraffin section, antigen retrieval by citric acid was carried out before immunostaining. Anti-TK (1:200) and anti-Luc (1:200) (both from Santa Cruz Biotechnology) primary antibodies were used to label TK-expressing hfBMSCs and Luc-expressing cancer cells in nude mice. Terminal deoxynucleotidyl transferase deoxyuridine triphosphate nick end labeling (TUNEL) assay (Calbiochem) was used to label apoptotic cell death *in vivo*. For the acquisition of hematoxylin and eosin, safranin O/fast green and immunohistochemical images, a Leica DMRB microscope (Leica DFC490 camera; Leica Application Suite Version

by bioluminescent imaging, in which the cytotoxicity was dependent on the ratio of SV40-TK-hfBMSCs to the cancer cells. (D) Immunogenicity was determined by mixed lymphocyte reaction. Lymphocytes from healthy donors showed a positive response toward haBMSCs with or without a short period of induction and toward hfBMSCs with a short period of osteogenic or adipogenic induction. $^*P < 0.05$, $^{**}P < 0.01$, $^{***}P < 0.001$, indicating significantly different groups (n = 4).

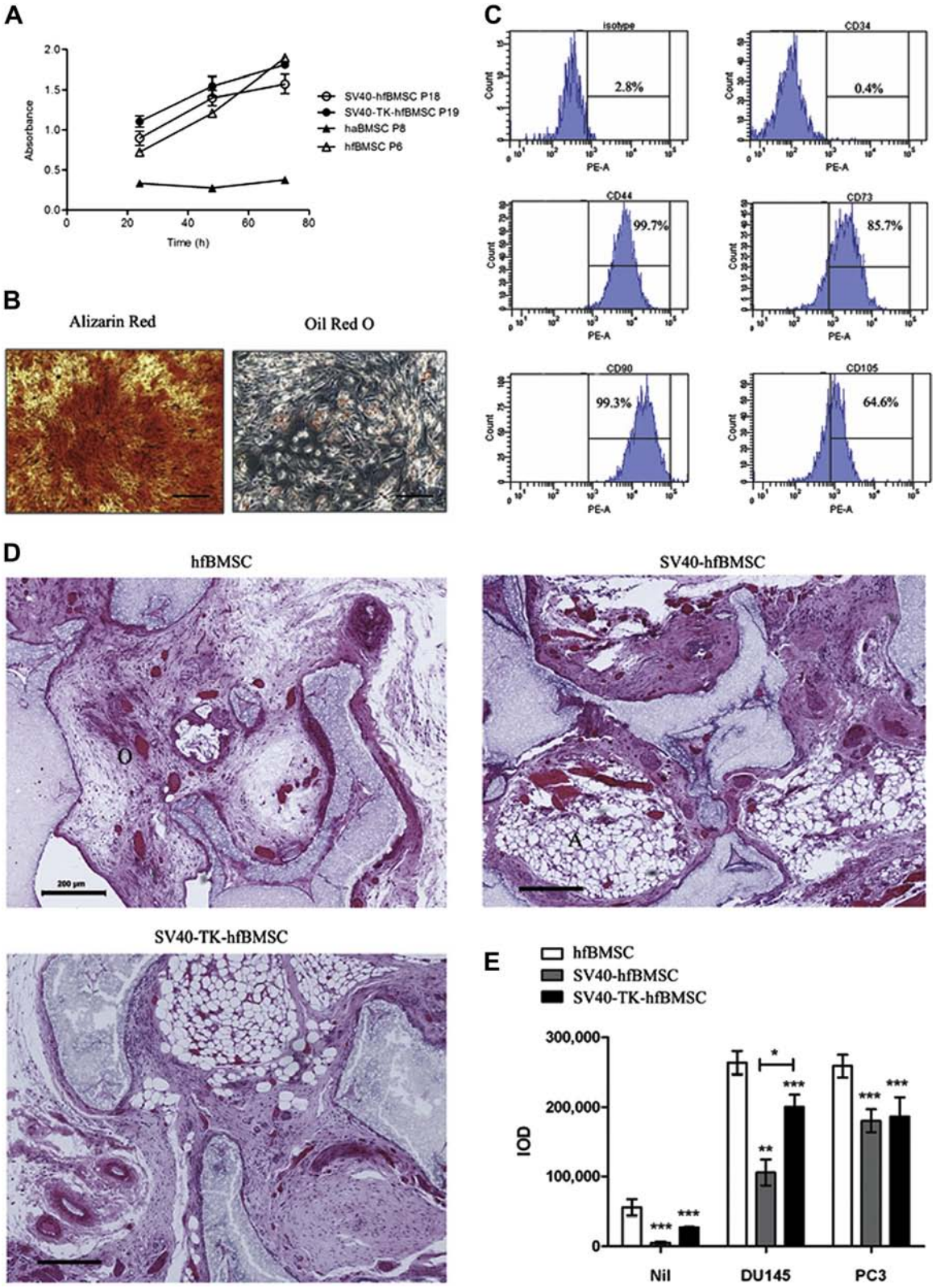

Figure 4. Stem cell properties of SV40-TK-hfBMSCs and assessment of their tumor-tropic migration ability. (A) hfBMSCs (P8), SV40-hfBMSCs (P18) and SV40-TK-hfBMSCs (P19) showed similar proliferation rate as indicated by BrdU assay. haBMSCs (P6) had comparatively the slowest proliferation. (B) Representation of osteogenic and adipogenic differentiated SV40-TK-hfBMSCs after induction. (Scale bar = 50 μm.) (C) Positive CD markers in hfBMSCs were retained in SV40-TK-hfBMSCs. (D) Hematoxylin and eosin

3.0.0 software; Leica Microsystems Cambridge Ltd, Cambridge, UK) was used. A Leica DMRXA2 was used for the acquisition of immunofluorescence images (Leica DC500 camera; Leica QWin software; Leica Microsystems Cambridge Ltd). Multi-color fluorescent images were acquired from a single capture. Staining of alizarin red and oil red O and GFP expression in cell culture were acquired by a Leica DMIRB microscope (Moticam 2300 camera; Motic Images Plus 2.0 ML software; Leica Microsystems Cambridge Ltd).

Statistics

Statistical analysis of raw data was performed by either one-way analysis of variance followed by Tukey post hoc test or Student *t*-test where appropriate. Counting of migrated cells in transwell assay was determined by Image Pro (MediaCybernetics). All results were presented as means ± SD. P value < 0.05 was considered statistically significant.

Results

Transduction of SV40 and TK into hfBMSCs

hfBMSCs were isolated and cultured in a clean room that was subjected to sterility tests, including endotoxin test (Limulus Amebocyte Lysate Kinetic; Lonza) and PCR Mycoplasma Detection (TaKaRa Biotechnology) (data not shown), before any subsequent experiments. MSCs with negative mycoplasm polymerase chain reaction and endotoxin level <0.25 EU/mL were cryopreserved in our Stem Cell Bank for later use. Single colony-forming assay and BrdU incorporation assay indicated higher self-renewal and proliferation rate of hfBMSCs (Figure 1A,B). hfBMSCs and haBMSCs had a similar profile of surface phenotype (Figure 1C). Three-dimensional pellet culture showed a lower content of proteoglycan in hfBMSC pellets, which indicated lower chondrogenic differentiation ability, whereas hfBMSCs and haBMSCs exhibited similar osteogenic and adipogenic differentiation potential (Figure 1D). SV40 and TK genes were transduced into hfBMSCs by lentiviruses in a stepwise manner. The transgenes were packed in 293FT cells. Single colonies of SV40-expressing hfBMSCs (Figure 2A) were identified and selected to expand further *in vitro*. Expression of SV40 in each subclone was confirmed by Western blot (Figure 2C). Repeated lentiviral transduction was done on these subclones to introduce TK-GFP into the genome. Single colonies with GFP signal were selected (Figure 2B). hfBMSCs subclone 4 with stable SV40 and TK expression were identified and expanded *in vitro* and used in subsequent experiments (Figure 2D).

TK-GCV-induced cytotoxicity in vitro

GCV induced cytotoxicity in SV40-TK-hfBMSCs in a concentration-dependent manner after 6 days of treatment (Figure 3A); this indicated the functional activity of TK in the SV40-TK-hfBMSCs. A strong correlation ($r^2 = 0.9536$) (Figure 3B) was found between the result of the live *in vivo* imaging (average radiance) and the MTT assay (absorbance at 570 nm). IVIS 200 was used to evaluate luciferase activity to determine the response of luciferase-expressing cancer cell lines co-cultured with SV40-TK-hfBMSCs to GCV. Luc-GFP-DU145 or Luc-GFP-PC3 cells alone were treated with GCV at various concentrations (0 μg/mL, 0.1 μg/mL, 1 μg/mL, 10 μg/mL, 50 μg/mL and 100 μg/mL) for 6 days. In the co-culture system, different ratios of Luc-GFP-DU145 or Luc-GFP-PC3 to SV40-TK-hfBMSCs (1:5, 1:1 and 5:1) were tested. The cytotoxicity increased significantly with decreased ratio at all tested concentrations (Figure 3C). The susceptibility of the tested cancer cells to TK-GCV suicide gene therapy was different. Luc-GFP-DU145 was more sensitive to MSC-GCV treatment. In contrast to in Luc-GFP-PC3 cells, GCV at 50 μg/mL and 100 μg/mL induced significant cytotoxic effect in Luc-GFP-DU145 cells ($P < 0.001$). Although GCV at 10 μg/mL, 50 μg/mL and 100 μg/mL induced similar cytotoxicity in SV40-TK-hfBMSCs alone, its cytotoxic effect was concentration dependent in the co-culture system. A higher GCV concentration was required to induce significant cytotoxic effect in higher ratios of cancer cells to SV40-TK-hfBMSCs.

Immunogenicity of hfBMSCs

The responses of lymphocytes culture of two healthy recipients to hfBMSCs and SV40-TK-hfBMSCs were tested by mixed lymphocyte reaction. A lower proliferation rate of the lymphocytes is associated with good transplant survival (i.e., lower tissue rejection and prolonged survivability of the cells). hfBMSCs

staining of hfBMSCs with or without transduction after 8 weeks of transplantation in HA/TCP scaffold in nude mice. Reddish osteoid tissues (O) and adipocytes (A) were noted. No fibrosarcoma-like tissue was noted. Representatives from three independent transplants. (Scale bar = 200 μm.) (E) Transwell migration assay indicated the positive response of hfBMSCs with or without transduction toward human prostate cancer cell lines *in vitro*. *$P < 0.05$, **$P < 0.01$, ***$P < 0.001$, indicating significantly different groups. Data were from five randomized fields of view.

significantly stimulated lymphocyte proliferation with or without a short period of osteogenic, adipogenic or chondrogenic induction (7 days of induction before the reaction). However, SV40-TK-hfBMSCs were less potent in terms of stimulating lymphocyte proliferation. Significant lymphocyte proliferation was stimulated only after prior osteogenic and adipogenic induction (Figure 3D).

Effects of SV40 and TK on MSC properties

Stem cell properties of hfBMSCs after SV40 and TK transduction were evaluated. BrdU assay indicated a similar proliferation rate before and after transduction (Figure 4A). SV40-TK-hfBMSCs were still able to differentiate in response to osteogenic or adipogenic induction medium (Figure 4B). Similar surface phenotypes ($CD34^-$, $CD44^+$, $CD73^+$, $CD90^+$ and $CD105^+$) were detected on the transduced cells (Figure 4C). The multilineage differentiation potential of the non-transduced or transduced hfBMSCs *in vivo* was compared using MSC preloaded-HA/TCP scaffold in nude mice (Figure 4D). From the hfBMSC 8-week transplants, reddish osteoids, light pinkish fiber matrices and adipocytes were found. A similar phenomenon was found in SV40-hfBMSC and SV40-TK-hfBMSC 8-week transplants. No detectable cartilage was found in any transplants by safranin O/fast green staining, and no tumor-like tissues were found in any of the transplants. The tumor-tropic migratory properties of the non-transduced and transduced hfBMSCs were tested by transwell assay (Figure 4E). hfBMSCs exhibited migratory property through the transwell membrane in the absence of cancer cells, which was reduced after being transduced ($P < 0.001$). In the presence of Luc-GFP-DU145 or Luc-GFP-PC3, the migratory ability increased remarkably by 5-fold in hfBMSCs and more in transduced hfBMSCs. SV40-hfBMSCs and SV40-TK-hfBMSCs had comparable migratory ability toward the PC3 cells, whereas transduction of TK restored the migratory ability of SV40-hfBMSCs toward the DU145 cells. Taken together, the transduction of both SV40 and TK did not interfere with the stem cell characteristics of hfBMSCs except that less osteoid formation was noticed *in vivo*.

SV40-TK-hfBMSCs and GCV system inhibited tumor growth in vivo

Nude mice bearing either Luc-GFP-DU145 or Luc-GFP-PC3 cells were subjected to treatment with GCV (30 mg/kg intraperitoneally), doxorubicin (Dox) (1.5 mg/kg intraperitoneally) or SV40-TK-hfBMSCs (1×10^6 cells/kg intravenously) followed by GCV (30 mg/kg intraperitoneally). Tumor volume, luciferase activity and weight were measured. For the DU145 group (Figure 5A), tumor growth was suppressed in Dox and TK-GCV groups as indicated by both tumor volume and luciferase activity. However, mice were vulnerable to Dox treatment as their weights declined over the treatment period. About 25% weight loss was noted at day 51 after Luc-GFP-DU145 injection, which was classified as substantial severity in our institute, and the mice were sacrificed accordingly. Despite the fact that there was no significant difference among the weights of the GCV group and TK-GCV group, the mice from the GCV group might have experienced reduced weight gain if the weight of tumor was taken into account. For the PC3 group (Figure 5B), tumor growth was noticed in GCV and Dox groups. However, the growth was later suppressed in the Dox group after the third treatment, although it was not statistically significant. For the TK-GCV group, four out of five mice were found to have no observable tumor on the back, and one of the mice died of suffocation when placed in the mice restrainer for MSC injection. The only exception had tumor growth even greater than the GCV group and was not included in the figure and marked. *In vivo* imaging indicated that the luciferase activity of the Dox group decreased and remained steady after the first round of treatment. Remarkable weight loss in the mice from the Dox group indicated they were vulnerable to Dox treatment. Injected SV40-TK-hfBMSCs were able to convert GCV into a cytotoxic compound in the tumor site to inhibit tumor growth without adverse effects on body weight as found in the Dox group. The luciferase activity was identified as bioluminescence by IVIS 200 imaging (Figure 5C). Representative images showed viable Luc-GFP-DU145 and Luc-GFP-PC3 cancer cell lines at an early time point. The presence of SV40-TK-hfBMSCs in tumor sites was confirmed by immunohistochemistry imaging (Figure 6A–F). Frozen sections of mice from the DU145 group with SV40-TK-hfBMSCs injection only were subjected to immunofluorescent staining to indicate the co-localization of SV40-TK-hfBMSCs and Luc-GFP-DU145 cells at the tumor site. Results showed the presence of SV40-TK-hfBMSCs proximal to Luc-GFP-DU145 cells. The frozen sections were fixed and subjected to immunohistochemistry for TK (Figure 6C,F) to reveal the surrounding architecture of the SV40-TK-hfBMSCs. Results indicated a more compact cell mass in DU145 tumors, whereas the architecture was much looser in the PC3 tumors. The injected SV40-TK-hfBMSCs grew in a compact organization inside DU145 tumors but dispersed inside PC3 tumors. TUNEL assay indicated apoptotic cell death in the tumor site of the DU145 group collected

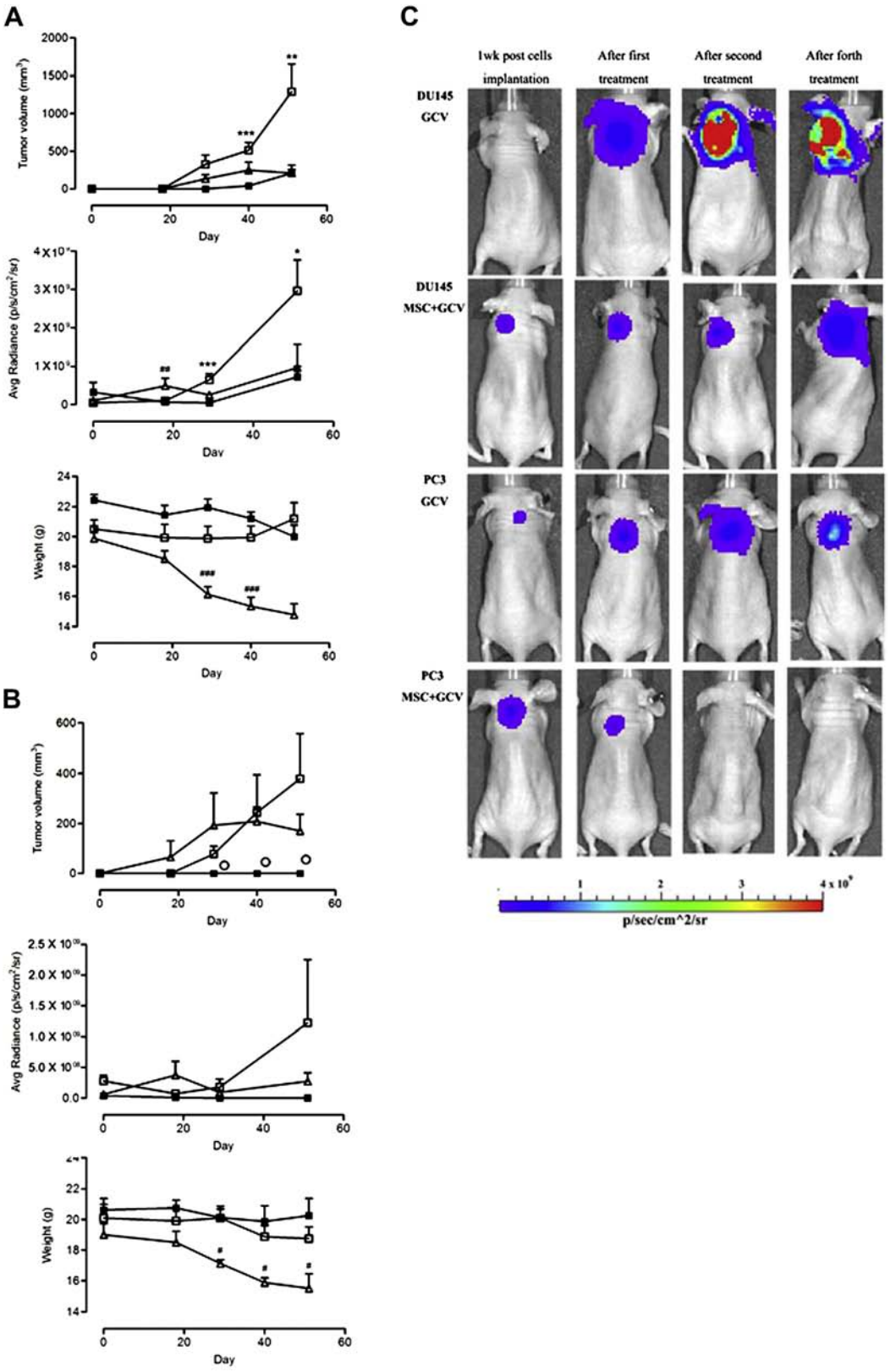

Figure 5. Anti-tumor effect of SV40-TK-hfBMSCs/GCV treatment in tumor xenograft animal model. Anti-tumor effect in DU145 group (n = 7) (A) or in PC3 group (n = 5, one outliner is shown as circle) (B) as indicated by tumor volume measurement and *in vivo* live bioluminescent imaging. Weighting was done to indicate the side effects present. The treatment was as effective as Dox in inhibiting tumor growth but without rendering any side effects on animals' weights. (C) Representative bioluminescent images were acquired by IVIS 200.

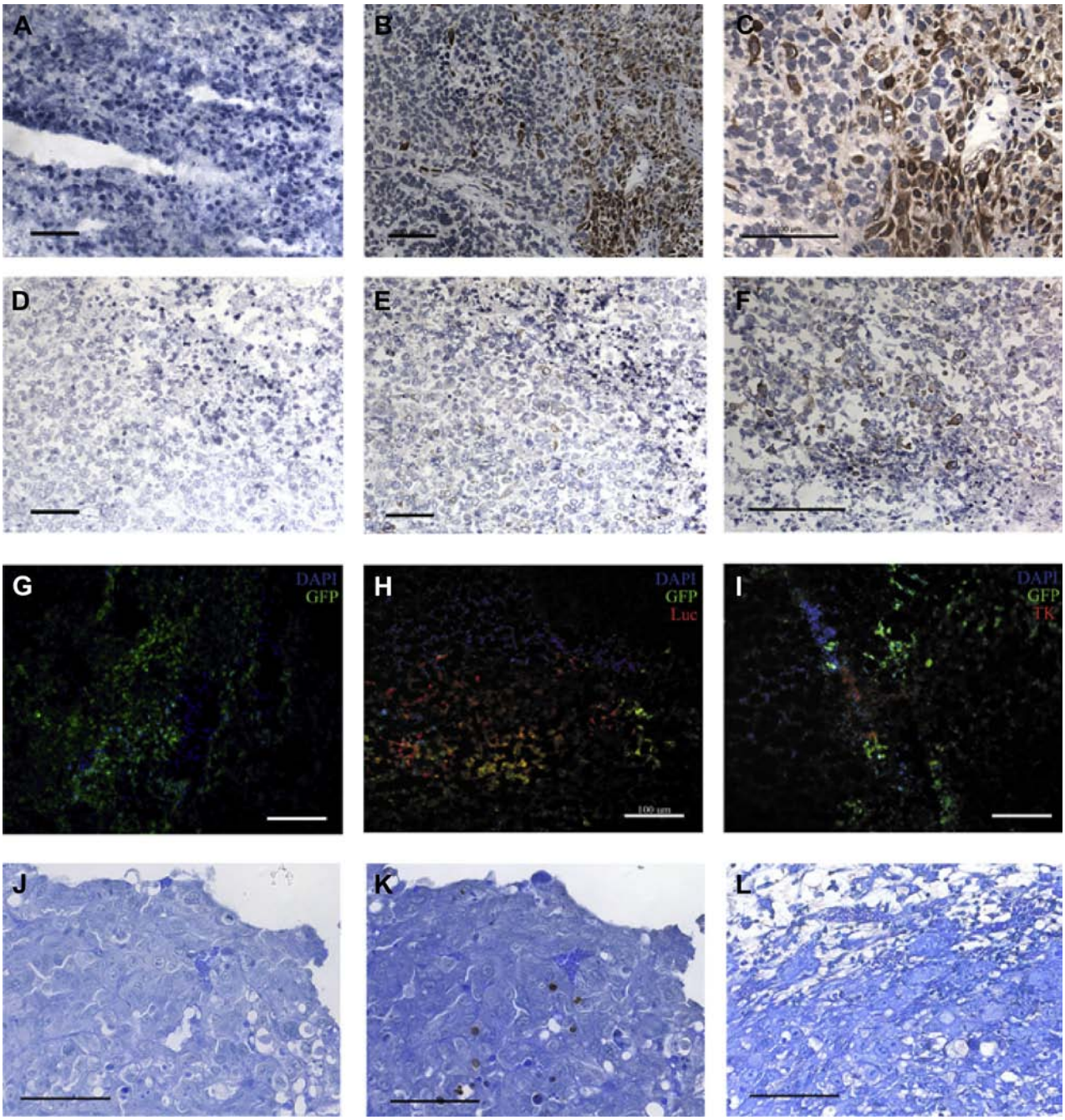

Figure 6. (A–L) Immunostaining of SV40-TK-hfBMSCs after intravenous injection and TUNEL assay. Intravenously injected SV40-TK-hfBMSCs in nude mice bearing Luc-GFP-DU145 (B, C) or Luc-GFP-PC3 (E, F) were located by immunostaining. (H) Fluorescent staining of Luc-GFP-DU145 in tumor. DAPI stain indicates the invasion of non-Luc-expressing host cells. (I) Co-localization of SV40-TK-hfBMSCs and Luc-GFP-DU145 was found inside the tumor. (K) TUNEL assay indicates apoptotic cell death after treatment. (L) No apoptotic cell death was found in GCV group. (A, D, G, J) Corresponding negative controls for immunostaining. Representation was from three independent experiments. (Scale bar = 100 μm.)

at the end of treatment (Figure 6K). SV40-TK-hfBMSCs were not found because the cells were eliminated by the administration of GCV. Nevertheless, these data suggest that reduction in tumor mass in TK/GCV group was associated with apoptotic cell death. The potential of accumulation of intravenously injected SV40-TK-hfBMSCs to organs, including liver, kidney, spleen, lung and heart, with massive blood supply was determined by hematoxylin and eosin staining and immunostaining of TK. Results showed normal tissue structures in these organs at the end of the treatment regimen (see supplementary

Figures 1,2), which implied the safety of this TK/GCV treatment protocol via systemic administration.

Discussion

The therapeutic potential of MSCs expressing TK for anti-tumor therapy has been reported using MSCs derived from human adult adipose tissue, human embryonic stem cell lines and human induced pluripotent stem cells (12,28,29). In line with these, our study has demonstrated the feasibility of using MSCs derived from human fetal bone marrow for gene therapy. The main advantage of fetal BMSCs over adult BMSCs is the prolonged life span *in vitro*, which allows time-consuming enrichment of the transduced MSCs with constitutive expression of desired transgene via single colony selection. The present study showed that the transduction of SV40 in addition to TK did not abolish the therapeutic effect of the cells. A previous study showed that murine BMSCs at passage 54 exhibited spontaneous malignant transformation in nude mice as indicated by acquired proliferation and formation of colonized fibrosarcoma in multiple organs after intravenous injection (30). In the present study, no observable colonized fibrosarcoma-like cell mass was found in various organs after SV40-TK-hfBMSCs/GCV treatment and in HA/TCP scaffold or injection in nude mice (see supplementary Figure 3). This result agreed with a previous study in which BMSCs from inbred pigs transfected with SV40 did not induce tumorigenicity (31). Nevertheless, the potential tumorigenicity of MSCs, particularly after a prolonged *in vitro* culture over passage 50, should be taken into consideration in future clinical studies. Compared with conventional chemotherapy, MSC suicide gene therapy had no significant adverse effect on the weight gain of the animals. Such safety and efficacy implies a great potential of immortalized MSC cell line expressing transgenes of interest for biologic study or clinical application. Despite the ready availability of human adult MSCs in various tissues, there is reluctance to use autologous MSCs from patients with osteogenesis imperfecta or tumors because of the genetic defeats. Allogeneic MSCs are an alternative, but immuno-compatibility is always of concern. Also, the transduction of MSCs and subsequent sterility and identity tests require well-trained personnel and accredited premises (i.e., Good Manufacturing Practices facilities), which are not commonly available in many medical centers.

Although it has been suggested that systemic injected MSCs might be entrapped passively in highly vascularized tissues, most likely in lung (32), our results demonstrated that hfBMSCs-TK/GCV treatment did not induce observable tissue damage in lung and other organs. The homing ability of MSCs has been shown to be affected by passage number and high confluence (33,34), so SV40-TK-hfBMSCs were subjected to subculture at 60−70% confluence to avoid loss of homing-associated proteins. Although cytomegalovirus (CMV) promoter is one of the most commonly used promoters for controlling the expression of transgenes in mammalian cells, silencing of the transgenes *in vivo* and *in vitro*, independent of species and transduction strategies, has been documented (35−38). The silencing is generally noticed $\geq$2 weeks after implantation *in vivo*. Methylation of CpG in the promoter region is the major gene suppression mechanism for the CMV promoter-driven transgene expression (39). In this study, the cells were used at passage number 22 or before with noticeable GFP signal. Also, this suicide gene therapy is less vulnerable to transgene silencing because the SV40-TK-hfBMSCs were allowed to stay *in vivo* for 3 days only, then GCV was given to elicit the cytotoxicity. Replacing the CMV promoter with human elongation factor-1 alpha (Ef1a) promoter could be a solution to such silencing in MSCs without significant influence on stem cell viability and adipogenic differentiation (40).

At the dosage of 1×10^6 cells/kg given in four repeated injection cycles, the treatment significantly inhibited the tumor growth in a xenograft model in nude mice. The dosage is similar to current clinical practices for the treatment of graft-versus-host disease (7) and much less than previous similar TK-MSC studies, in which 0.5−1 million cells were injected per mice. Our data suggest that injection of low numbers of MSCs in a repeated manner could exhibit a comparable therapeutic effect as single injection of a high number of MSCs. It is speculated that the functional outcome of systemic injection of MSCs is not cell number and may reach a plateau beyond additional injection of MSCs (41). There is no guideline at the present time on the dosage of systemic injected MSCs as drugs in pharmaceutical sciences because the cellular kinetics of injected MSCs is not well elucidated. The number and duration of MSC expressing suicide genes at the tumor sites would be an important determining factor for the therapeutic outcome. Given that MSCs were previously shown to possess modulatory effects on tumor cells and neovascularization (15,42,43), the monitoring of the fate of the MSCs would provide information on the design of a treatment regimen. TK and its radiolabeled nucleoside analogous, such as 2'-deoxy-2'-^{18}F-fluoro-5-ethyl-1-β-D-arabinofuranosyl-uracil (^{18}F-FEAU) has been widely used in reporter gene combined positron emission tomography and computed tomography

imaging (44). In clinical practice, the distribution of the systemic injected SV40-TK-hfBMSCs could be determined before GCV administration, allowing justification of the dosage of TK-MSCs and pre-treatment period.

In this study, SV40-TK-hfBMSCs/GCV treatment was effective in suppressing tumor growth at an early stage. However, poor diagnosis of tumor makes early detection difficult and is the major hindrance to conventional anti-tumor therapy. The tumor site is generally highly vascularized at a later stage (45), and the cytokines released by tumors, such as vascular endothelial cell growth factor, recruit MSCs (46). Two measures have been proposed to promote MSC suicide gene therapy against late-stage tumor. One measure is the administration of adjuvant, which increases the expression of gap junction proteins (47), but this approach does not increase the number of MSCs at the sites of interest, and the involvement of gap junction in MSC suicide gene therapy is not well elucidated yet. Another measure is to induce further inflammation at the tumor sites by some means so as to promote MSC homing. The second measure is clinically more relevant because current site-specific irradiation induces death of tumor cells and surrounding cells, which leads to inflammation and cytokine release (48). Chemotherapy generally is not an appropriate candidate to boost up MSC suicide gene therapy because of possible systemic inflammation and cytotoxicity to the MSCs as well. However, the diverse classes of therapeutic drugs, with different underlying mechanisms, lead to the interaction with MSC suicide gene therapy in a synergistic manner. Chemoembolization is practically feasible to introduce site-specific chemotherapy. Tumor-specific target delivery is another option, although elucidation of this option is required. Our group is studying whether local injection of chemotherapeutic could promote MSC suicide gene treatment. These studies would shed light on developing combination therapy to enhance the efficacy of MSC suicide gene treatment.

In conclusion, this study provides the first evidence showing the anti-tumor effect of immortalized hfBMSCs expressing TK. Further investigations on chromosomal stability and optimized dosage of MSC injection are needed to provide pre-clinical safety assessment before moving on to clinical trials.

Acknowledgments

The authors thank Li Ka Shing Institute of Health, The Chinese University of Hong Kong, for providing the use of clean room human cell culture facilities, and Miss Nina Chu for help in clinical specimen collection. This study was supported by an Innovation and Technology Fund of Hong Kong SAR (ITS/305/09) to Gang Li and Kai-Ming Chan and a grant from National Natural Science Foundation of China (NSFC No. 81172177) to Gang Li.

Disclosure of interest: The authors have no commercial, proprietary, or financial interest in the products or companies described in this article.

References

1. Javazon EH, Beggs KJ, Flake AW. Mesenchymal stem cells: paradoxes of passaging. Exp Hematol. 2004;32:414–25.
2. Caplan AI. Why are MSCs therapeutic? New data: new insight. J Pathol. 2009;217:318–24.
3. Rastegar F, Shenaq D, Huang J, Zhang W, Zhang BQ, He BC, et al. Mesenchymal stem cells: molecular characteristics and clinical applications. World J Stem Cells. 2010;2:67–80.
4. Rossignol J, Boyer C, Thinard R, Remy S, Dugast AS, Dubayle D, et al. Mesenchymal stem cells induce a weak immune response in the rat striatum after allo or xenotransplantation. J Cellular Mol Med. 2009;13:2547–58.
5. Popp FC, Renner P, Eggenhofer E, Slowik P, Geissler EK, Piso P, et al. Mesenchymal stem cells as immunomodulators after liver transplantation. Liver Transpl. 2009;15:1192–8.
6. Gerdoni E, Gallo B, Casazza S, Musio S, Bonanni I, Pedemonte E, et al. Mesenchymal stem cells effectively modulate pathogenic immune response in experimental autoimmune encephalomyelitis. Ann Neurol. 2007;61:219–27.
7. Lin Y, Hogan WJ. Clinical application of mesenchymal stem cells in the treatment and prevention of graft-versus-host disease. Adv Hematol. 2011;2011:427863.
8. Qiao L, Xu ZL, Zhao TJ, Ye LH, Zhang XD. Dkk-1 secreted by mesenchymal stem cells inhibits growth of breast cancer cells via depression of Wnt signalling. Cancer Lett. 2008;269:67–77.
9. Khakoo AY, Pati S, Anderson SA, Reid W, Elshal MF, Rovira II, et al. Human mesenchymal stem cells exert potent antitumorigenic effects in a model of Kaposi's sarcoma. J Exp Med. 2006;203:1235–47.
10. Shah K. Mesenchymal stem cells engineered for cancer therapy. Adv Drug Deliv Rev. 2012;64:739–48.
11. Nicholas TW, Read SB, Burrows FJ, Kruse CA. Suicide gene therapy with Herpes simplex virus thymidine kinase and ganciclovir is enhanced with connexins to improve gap junctions and bystander effects. Histol Histopathol. 2003;18:495–507.
12. Kucerova L, Altanerova V, Matuskova M, Tyciakova S, Altaner C. Adipose tissue-derived human mesenchymal stem cells mediated prodrug cancer gene therapy. Cancer Res. 2007;67:6304–13.
13. Ramos CA, Asgari Z, Liu E, Yvon E, Heslop HE, Rooney CM, et al. An inducible caspase 9 suicide gene to improve the safety of mesenchymal stromal cell therapies. Stem Cells. 2010;28:1107–15.
14. Song C, Xiang J, Tang J, Hirst DG, Zhou J, Chan KM, et al. Thymidine kinase gene modified bone marrow mesenchymal stem cells as vehicles for antitumor therapy. Hum Gene Ther. 2011;22:439–49.
15. Spaeth EL, Dembinski JL, Sasser AK, Watson K, Klopp A, Hall B, et al. Mesenchymal stem cell transition to tumor-associated fibroblasts contributes to fibrovascular network expansion and tumor progression. PLoS One. 2009;4:e4992.
16. Suzuki K, Sun R, Origuchi M, Kanehira M, Takahata T, Itoh J, et al. Mesenchymal stromal cells promote tumor growth through the enhancement of neovascularization. Mol Med. 2011;17:579–87.

17. Zhu W, Huang L, Li Y, Qian H, Shan X, Yan Y, et al. Mesenchymal stem cell-secreted soluble signaling molecules potentiate tumor growth. Cell Cycle. 2011;10:3198–207.
18. Miletic H, Fischer Y, Litwak S, Giroglou T, Waerzeggers Y, Winkeler A, et al. Bystander killing of malignant glioma by bone marrow-derived tumor-infiltrating progenitor cells expressing a suicide gene. Mol Ther. 2007;15:1373–81.
19. Zischek C, Niess H, Ischenko I, Conrad C, Huss R, Jauch KW, et al. Targeting tumor stroma using engineered mesenchymal stem cells reduces the growth of pancreatic carcinoma. Ann Surg. 2009;250:747–53.
20. Matuskova M, Hlubinova K, Pastorakova A, Hunakova L, Altanerova V, Altaner C, et al. HSV-tk expressing mesenchymal stem cells exert bystander effect on human glioblastoma cells. Cancer Lett. 2010;290:58–67.
21. Niess H, Bao Q, Conrad C, Zischek C, Notohamiprodjo M, Schwab F, et al. Selective targeting of genetically engineered mesenchymal stem cells to tumor stroma microenvironments using tissue-specific suicide gene expression suppresses growth of hepatocellular carcinoma. Ann Surg. 2011;254:767–74.
22. Kawano Y, Kobune M, Yamaguchi M, Nakamura K, Ito Y, Sasaki K, et al. Ex vivo expansion of human umbilical cord hematopoietic progenitor cells using a coculture system with human telomerase catalytic subunit (hTERT)-transfected human stromal cells. Blood. 2003;101:532–40.
23. Bentzon JF, Stenderup K, Hansen FD, Schroder HD, Abdallah BM, Jensen TG, et al. Tissue distribution and engraftment of human mesenchymal stem cells immortalized by human telomerase reverse transcriptase gene. Biochem Biophys Res Commun. 2005;330:633–40.
24. Huang E, Bi Y, Jiang W, Luo X, Yang K, Gao JL, et al. Conditionally immortalized mouse embryonic fibroblasts retain proliferative activity without compromising multipotent differentiation potential. PLoS One. 2012;7:e32428.
25. Guillot PV, Gotherstrom C, Chan J, Kurata H, Fisk NM. Human first-trimester fetal MSC express pluripotency markers and grow faster and have longer telomeres than adult MSC. Stem Cells. 2007;25:646–54.
26. Kutner RH, Zhang XY, Reiser J. Production, concentration and titration of pseudotyped HIV-1-based lentiviral vectors. Nat Protoc. 2009;4:495–505.
27. Lee WY, Lui PP, Rui YF. Hypoxia-mediated efficient expansion of human tendon-derived stem cells in vitro. Tissue Eng. 2012;18:484–98.
28. Zhao Y, Lam DH, Yang J, Lin J, Tham CK, Ng WH, et al. Targeted suicide gene therapy for glioma using human embryonic stem cell-derived neural stem cells genetically modified by baculoviral vectors. Gene Ther. 2011;19:189–200.
29. Yang J, Lam DH, Goh SS, Lee EX, Zhao Y, Tay FC, et al. Tumor tropism of intravenously injected human-induced pluripotent stem cell-derived neural stem cells and their gene therapy application in a metastatic breast cancer model. Stem Cells. 2012;30:1021–9.
30. Miura M, Miura Y, Padilla-Nash HM, Molinolo AA, Fu B, Patel V, et al. Accumulated chromosomal instability in murine bone marrow mesenchymal stem cells leads to malignant transformation. Stem Cells. 2006;24:1095–103.
31. Liu J, Lu XF, Wan L, Lu B, Li SF, Zeng YZ, et al. Immortalization of bone marrow mesenchymal stem cells from inbred pig for regenerative medicine. Key Eng Mater. 2005;288–289:43–6.
32. Karp JM, Leng Teo GS. Mesenchymal stem cell homing: the devil is in the details. Cell Stem Cell. 2009;4:206–16.
33. Rombouts WJ, Ploemacher RE. Primary murine MSC show highly efficient homing to the bone marrow but lose homing ability following culture. Leukemia. 2003;17:160–70.
34. De Becker A, Van Hummelen P, Bakkus M, Vande Broek I, De Wever J, De Waele M, et al. Migration of culture-expanded human mesenchymal stem cells through bone marrow endothelium is regulated by matrix metalloproteinase-2 and tissue inhibitor of metalloproteinase-3. Haematologica. 2007;92:440–9.
35. Palmer TD, Rosman GJ, Osborne WR, Miller AD. Genetically modified skin fibroblasts persist long after transplantation but gradually inactivate introduced genes. Proc Natl Acad Sci U S A. 1991;88:1330–4.
36. Loser P, Jennings GS, Strauss M, Sandig V. Reactivation of the previously silenced cytomegalovirus major immediate-early promoter in the mouse liver: involvement of NFkappaB. J Virol. 1998;72:180–90.
37. Radhakrishnan P, Basma H, Klinkebiel D, Christman J, Cheng PW. Cell type-specific activation of the cytomegalovirus promoter by dimethylsulfoxide and 5-aza-2′-deoxycytidine. Int J Biochem Cell Biol. 2008;40:1944–55.
38. Hickman MA, Malone RW, Lehmann-Bruinsma K, Sih TR, Knoell D, Szoka FC, et al. Gene expression following direct injection of DNA into liver. Hum Gene Ther. 1994;5:1477–83.
39. Yoder JA, Walsh CP, Bestor TH. Cytosine methylation and the ecology of intragenomic parasites. Trends Genet. 1997;13:335–40.
40. McGinley L, McMahon J, Strappe P, Barry F, Murphy M, O'Toole D, et al. Lentiviral vector mediated modification of mesenchymal stem cells and enhanced survival in an in vitro model of ischaemia. Stem Cell Res Ther. 2011;2:12.
41. Wu J, Sun Z, Sun HS, Weisel RD, Keating A, Li ZH, et al. Intravenously administered bone marrow cells migrate to damaged brain tissue and improve neural function in ischemic rats. Cell Transplant. 2008;16:993–1005.
42. Zhang Y, Daquinag AC, Amaya-Manzanares F, Sirin O, Tseng C, Kolonin MG. Stromal progenitor cells from endogenous adipose tissue contribute to pericytes and adipocytes that populate the tumor microenvironment. Cancer Res. 2012;72:5198–208.
43. Kucerova L, Matuskova M, Hlubinova K, Altanerova V, Altaner C. Tumor cell behaviour modulation by mesenchymal stromal cells. Mol Cancer. 2010;9:129.
44. Perin EC, Tian M, Marini FC 3rd, Silva GV, Zheng Y, Baimbridge F, et al. Imaging long-term fate of intramyocardially implanted mesenchymal stem cells in a porcine myocardial infarction model. PLoS One. 2011;6:e22949.
45. Hoeben A, Landuyt B, Highley MS, Wildiers H, Van Oosterom AT, De Bruijn EA. Vascular endothelial growth factor and angiogenesis. Pharmacol Rev. 2004;56:549–80.
46. Bergfeld SA, DeClerck YA. Bone marrow-derived mesenchymal stem cells and the tumor microenvironment. Cancer Metastasis Rev. 2010;29:249–61.
47. Ryu CH, Park KY, Kim SM, Jeong CH, Woo JS, Hou Y, et al. Valproic acid enhances anti-tumor effect of mesenchymal stem cell mediated HSV-TK gene therapy in intracranial glioma. Biochem Biophys Res Commun. 2012;421:585–90.
48. Francois S, Bensidhoum M, Mouiseddine M, Mazurier C, Allenet B, Semont A, et al. Local irradiation not only induces homing of human mesenchymal stem cells at exposed sites but promotes their widespread engraftment to multiple organs: a study of their quantitative distribution after irradiation damage. Stem Cells. 2006;24:1020–9.

Supplementary data

Supplementary data related to this article can be found online at http://dx.doi.org/10.1016/j.jcyt.2013.06.010